PASSIVE MARGIN EARTHQUAKES, STRESSES AND RHEOLOGY

SETH STEIN
Department of Geological Sciences
Northwestern University, Evanston IL 60208, USA

SIERD CLOETINGH
Institute of Earth Sciences,
University of Utrecht, 3584 CD Utrecht, The Netherlands

NORMAN H. SLEEP
Department of Geophysics,
Stanford University, Stanford CA 94305, USA

RINUS WORTEL
Institute of Earth Sciences,
University of Utrecht, 3584 CD Utrecht, The Netherlands

"Nearly all stable masses exhibit marginal features which are seismically active."
- *Seismicity of the Earth*, Gutenberg and Richter

ABSTRACT. The occurrence of large earthquakes on passive continental margins poses the challenge of explaining the causes of earthquakes not directly related to plate boundary processes. Here, we suggest several features of models for passive margin seismicity based on inferences from the distribution and mechanisms of seismicity in the zone along the Canadian Atlantic coast. The concentration of earthquakes *along* the margin suggests that they are related to the reactivation of faults remaining from the continental rifting. The variation in focal mechanisms *across* the margin suggests a spatially varying stress field. Although the later feature may not be a general characteristic, the empiricism that passive margin seismicity seems most evident on recently deglaciated margins suggests that deglaciation is at least partially responsible for the earthquakes.

Several sources of stress may contribute to passive margin seismicity. Flexural stresses due to the removal of ice loads, and spreading stresses due to the different densities of continental and oceanic lithosphere, can give stress differences of tens of MPa across a margin and normal to it. These stresses could cause the change from deviatoric compression landward to deviatoric extension seaward suggested by the Baffin Bay focal mechanisms. Stresses of comparable magnitude, but compressive everywhere, can result from the combination of integrated plate driving forces, "ridge push" and basal drag. The resultant compression direction can often be approximately normal to the margin.

Although these stresses can explain many features of passive margin seismicity, it is natural to ask what effects the major (~10 km) sediment loads along margins may have. These loads can give rise to flexural stresses of hundreds of MPa, an order of magnitude greater than anticipated from the other causes. These stresses might then be expected to dominate the others, giving rise to seismicity along all passive margins, with no preference for deglaciated ones. Similarly, local variations in sediment loading should at least partially mask the effects of the other stress sources.

We consider two possible explanations for this paradox, both based on the rheology of the passive margin lithosphere. In one model, the stresses due to long term sediment loading are relaxed since the lithosphere acts as a viscoelastic material. Simple calculations for a typical passive margin loading history, in which sediment is deposited over long periods of time throughout the margin's history, imply that the flexural stresses can be reduced by an order of magnitude. Only very rapid sedimentation allows stress to accumulate faster than it relaxes, suggesting that only in extreme cases can sediment loading result in seismicity. In the second model, due to the depth dependant rheology of the lithosphere, a brittle region overlying a ductile one, the flexural stresses are somewhat reduced, but seismicity occurs only in response to the recent stress increment. In this model the long term sediment load contributes to the stress but does not induce seismicity.

S. Gregersen and P. W. Basham (eds.), Earthquakes at North-Atlantic Passive Margins: Neotectonics and Postglacial Rebound, 231–259.

1. Introduction

Papers discussing passive continental margin seismicity typically begin by demonstrating that earthquakes of significant size can and do occur along such margins. These margins are "passive" in that they are not active plate boundaries, a criterion which does not preclude seismicity. The papers in this volume demonstrate the phenomenon for a variety of passive margins.

Although it is clear that earthquakes occur on passive margins, it is less obvious why they should. By definition, we cannot appeal to processes at active plate boundaries, which generate the overwhelming majority of global seismicity. Instead, possible explanations are traditionally posed in terms of the intraplate stresses acting at the margin. To test such explanations, we first review some observed aspects of the seismicity. We then review various sources of stress, discuss their relation to the seismicity, note possible difficulties, and suggest alternative explanations.

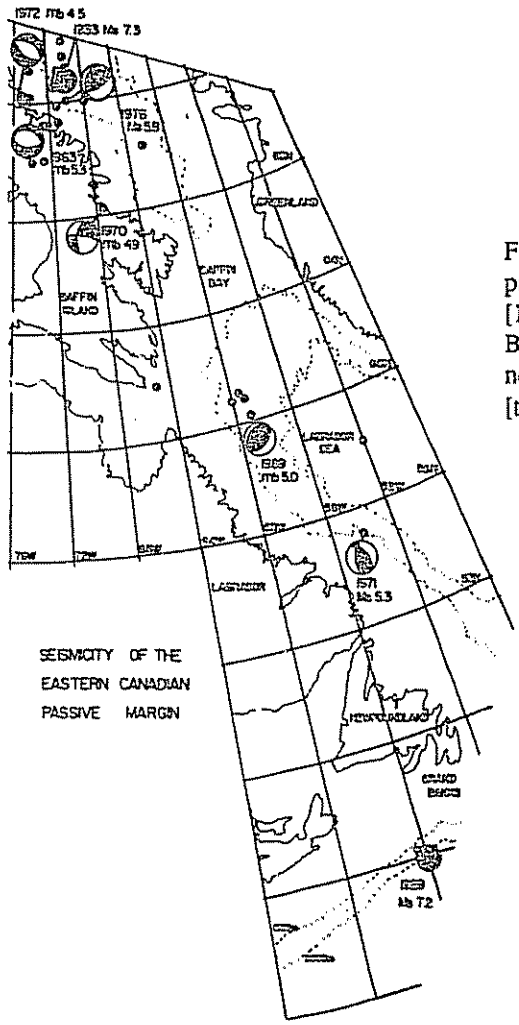

Figure 1: Seismicity of the eastern Canadian passive margin, compiled by Stein et al. [1979] with revised mechanism for 1933 Baffin Bay event [Sleep et al., 1988]. Figure not updated to include other recent studies [this volume].

The earthquakes along the passive margin of eastern Canada provide the type example for such seismicity, given the large earthquakes that occur there. This unusual concentration, most evident on the western margin of Baffin Bay, has been noted for some time [Gutenberg and Richter, 1954; Hashizume, 1973; Qamar, 1974; Basham et al., 1977]. A full review of this seismicity seems unnecessary here, given the papers in this volume by Adams and Basham and by Hasegawa and Hermann, but several points illustrated by Figure 1 are worth noting:

- Earthquake magnitudes can reach M_s 7, as in the 1933 Baffin Bay and 1929 Grand Banks events.
- Earthquakes occur along the length of the margin, and are concentrated near it.
- In the Baffin Bay region (Figure 2), earthquake focal mechanisms vary across the margin: the inland events show normal faulting and the seaward events show thrust faulting.

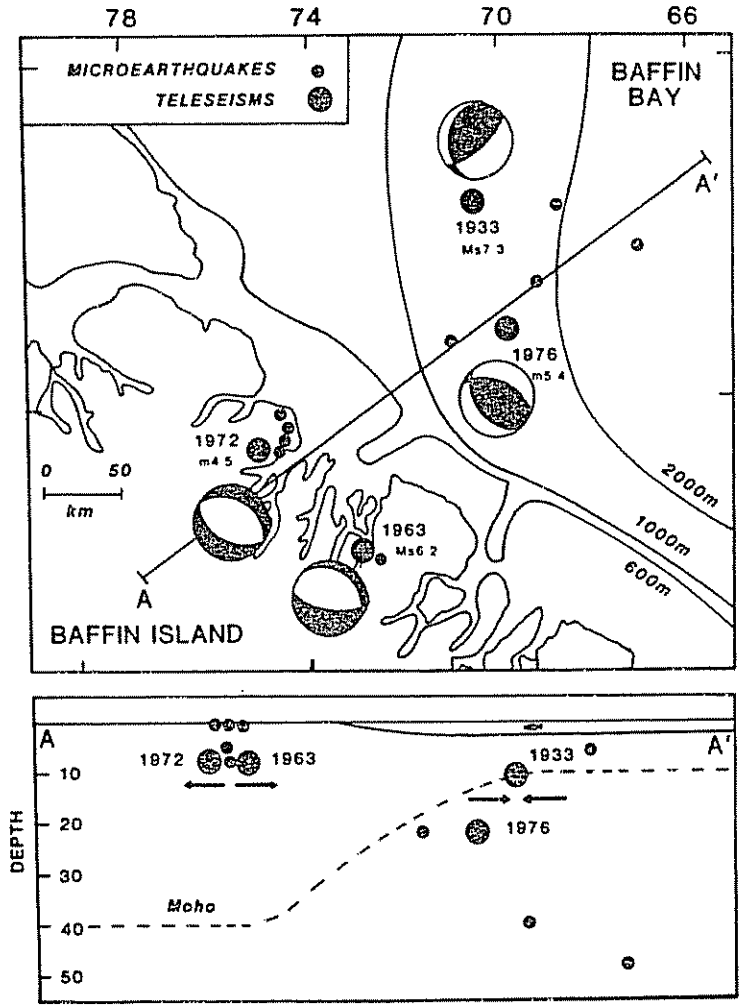

Figure 2: Seismicity of the Baffin Bay region, from Stein et al. [1979] and Sleep et al. [1988]. Microearthquakes and crustal structure from Reid and Falconer [1982].

These observations led to a model [Stein et al., 1979] in which the earthquakes were assumed to result from the flexural stresses generated by the removal of ice sheets which loaded the continental shelf. A subsequent paper [Sleep et al., 1988] expanded the analysis by incorporating the effect of continental margin spreading stress. These models were motivated by the

large passive margin earthquakes along the Canadian margin, and the suggestion that, in general, deglaciated margins are more seismically active. The seismicity of other margins, especially those of Fennoscandia, is discussed by many of the other papers in this volume. It appears that the deglaciated margins (Canada, Fennoscandia, Greenland) (Figure 3) have the larger passive margin earthquakes. The dataset available is not, however, large enough to conclusively demonstrate (or exclude) this.

In this paper, we review several mechanisms which can give rise to stresses at passive margins, and consider which would be expected at all margins and which are restricted to certain margins. Presumably, several effects act in concert to produce passive margin seismicity. A decision of which features to include in a model of passive margin seismicity depends on what effects are to be explained. In particular, if the apparent concentration of seismicity on deglaciated margins proves not to be a real effect, or the variation in focal mechanisms across the Baffin Bay margin proves to be a site-specific feature, stress mechanisms operative at most passive margins may be an adequate explanation for seismicity.

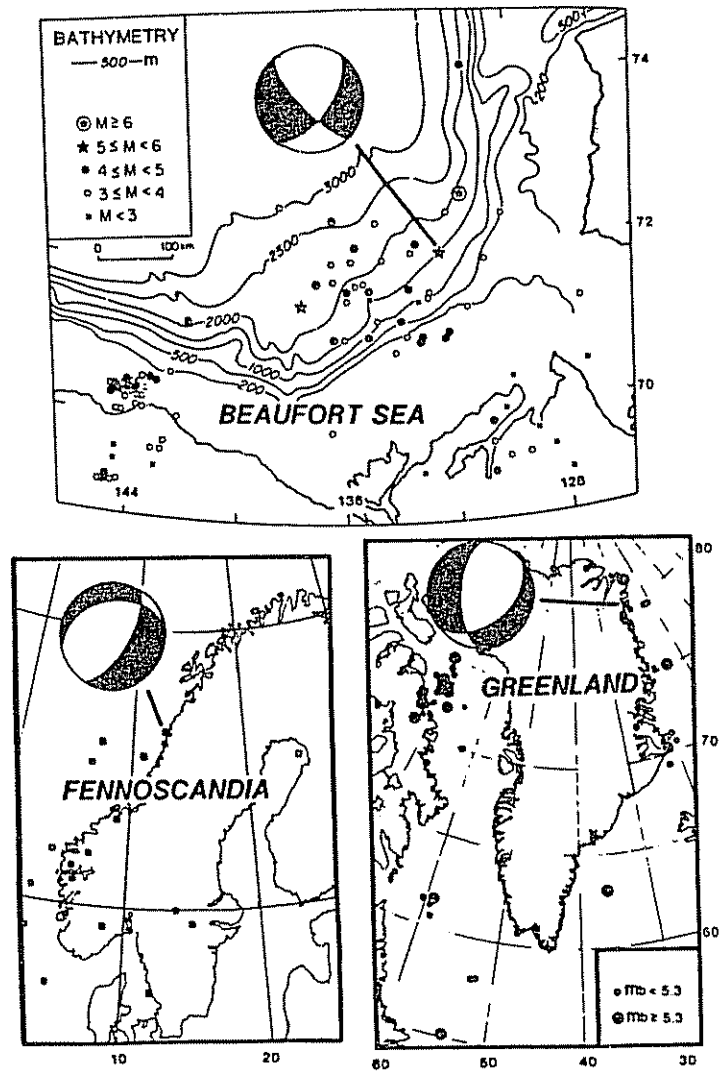

Figure 3: Seismicity of several other passive continental margins [Sleep et al., 1988]. Beaufort Sea seismicity (1920 - 1975) and focal mechanism of 6/14/75 event from Hasegawa et al. [1979]. Fennoscandian seismicity (1497 - 1975) from Husebye et al. [1978]; composite mechanism for 1978 swarm from Bungum et al. [1979]. Greenland seismicity from Sykes [1979]; mechanism of 11/26/71 event from Sykes and Sbar [1974]. More recent results for Fennoscandia, Greenland, and other margins are presented elsewhere in this volume.

2. Deglaciation flexure

In analyzing stresses due to deglaciation, we use the conventional model of elastic plate flexure [Turcotte and Schubert, 1982]. The displacement $w(x)$ resulting from a line load $P(x)$ is described by

$$D\frac{d^4w(x)}{dx^4} + kw(x) = P(x) \tag{1}$$

where $D = ET^3/12(1-\nu^2)$ is the flexural rigidity, ν is Poisson's ratio, T is the elastic lithospheric thickness, and E is Young's modulus. k is the density restoring force, equal to $g\,\rho_a$, the acceleration of gravity times the density of the material underlying the elastic plate or, for a load applied under water, $k = g(\rho_a - \rho_w)$, where ρ_w is the density of the water filling the depression created by the load. A variant on a solution for a semi-infinite load [Walcott, 1970], shows that removal of an ice sheet extending to $x=0$ ($P(x) = -hg\,\rho_i$ for $x<0$ and 0 for $x>0$) causes a displacement

$$w(x) = (-\rho_i h/2\rho_a)\, e^{-x/\alpha} \cos(x/\alpha) \qquad (x>0)$$
$$(-\rho_i h/2\rho_a)\,(2-e^{x/\alpha}\cos(x/\alpha)) \qquad (x<0) \tag{2}$$

Since displacement is defined as positive downward, uplift results (Figure 4) from removal of the load. The spatial variation of the displacement is given by the flexural parameter $\alpha = (4D/k)^{1/4}$. The equation can be formulated in slightly different ways, depending on the precise load geometry assumed. Here, the load height h is that in excess of the final unloaded water depth, and the restoring force is assumed not to include the water density, since the load originally rose above the sea surface. (This formulation is a simplification, since the flexural deflection is effectively under water on the seaward side, and on land on the continental side.) Away from the load edge, the displacement tends to that predicted by local isostasy, $\rho_i h/\rho_a$. The deviation from local isostasy reflects the finite strength of the lithosphere. Increased lithospheric strength, indicated by larger values of E and hence D, results in larger α and hence a broader flexure.

The corresponding flexural (or fiber) stress, at a vertical distance z measured upward from the center of the lithosphere ($T/2$), is

$$\sigma_{xx}(x,z) = \frac{-Ez}{(1-\nu^2)}\frac{d^2w(x)}{dx^2} = \frac{Ez\,\rho_i h}{(1-\nu^2)\,\alpha^2\,\rho_a}\, e^{-|x|/\alpha}\sin(x/\alpha) \tag{3}$$

(the $(1-\nu^2)$ term varies between authors depending on the geometry assumed). The plane $z=0$ is the neutral surface ($T/2$), where the stress is zero. Above the neutral surface, σ_{xx} is negative (tensional) for $x<0$ and positive (compressional) for $x>0$. Thus the deglaciated region should be in tension, and the unglaciated region in compression, as suggested by the focal mechanisms. Below the neutral surface, the stress reverses. Figure 4 shows that for a one km thick ice load, the rebound is several hundred meters, and the corresponding stresses (plotted at the top of the lithosphere) reach tens of MPa. Naturally, the precise values depend on the load assumed and the flexural rigidity, and thus implicitly for displacement and explicitly for stress, on lithospheric thickness and Young's modulus. For our purposes, we simply note that an ice load a few km thick will give flexural stresses of a few tens of MPa. These stresses, though not enough to fracture previously unfaulted lithosphere, could be adequate to induce faulting on faults remaining from the continental rifting.

A solution for arbitrary loads can be found using a Fourier series representation

$$P(x) = (P_0 / k) \sum_{n=0}^{\infty} C_n \cos(n \pi x / a), \tag{4}$$

which gives a flexural displacement

$$w(x) = (P_0 / k) \sum_{n=0}^{\infty} B_n C_n \cos(n \pi x / a) \tag{5}$$

where

$$B_n = 1 / [\, 1 + (D/k)(n\pi/a)^4 \,] = 1 / [\, 1 + (1/4)(\alpha n \pi/a)^4 \,] \tag{6}$$

shows how individual wavelengths respond. The longer wavelengths tend to the isostatic solution, $w(x) = (P_0 / k)$, since $B_n \rightarrow 1$ as $n \rightarrow 0$. Thus for load lengths shorter than a semi-infinite one, the deviation from local isostasy is greater.

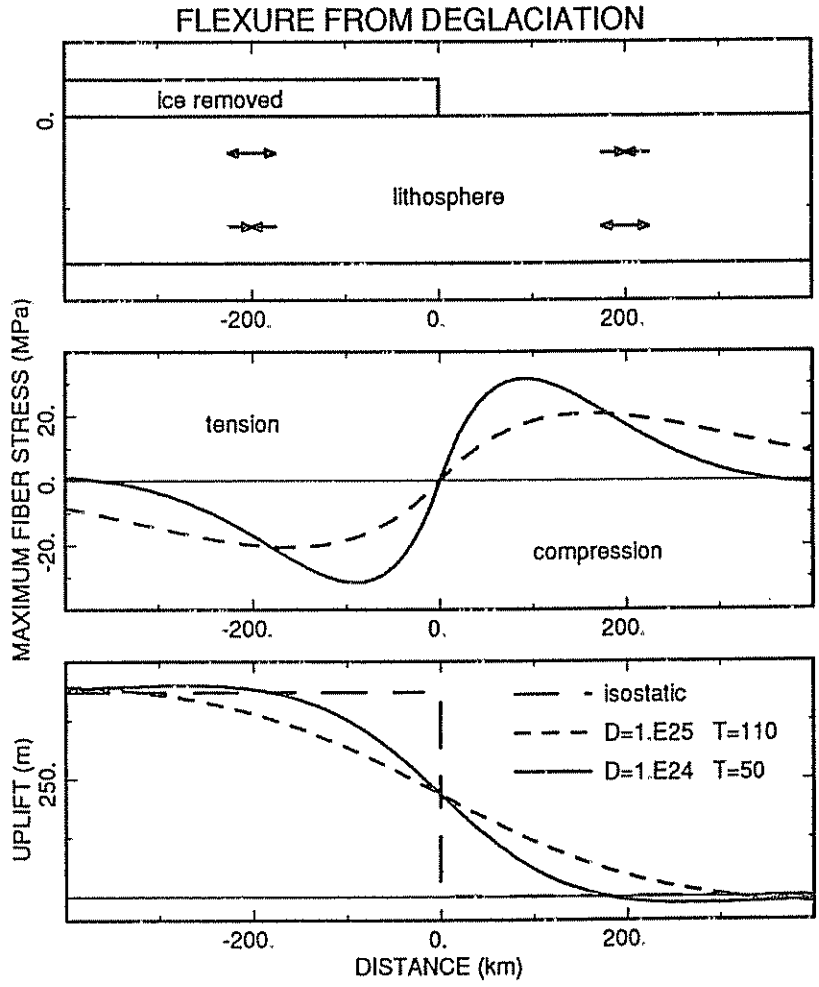

Figure 4: Schematic model for uplift and stresses resulting from flexure generated by the removal of a 1 km ice sheet from the continental shelf.

This analysis of deglaciation flexure is schematic and does not incorporate a variety of possible effects. In particular, it treats the lithosphere as having the same properties along and

across the margin, and neglects effects due to the non-two dimensional geometry of the margin and the load. As a result, we predict only in a general way the distribution of the stress, for example, the location of the change from compression to tension. Our purpose here, as in the discussion of the other stresses, is to characterize the magnitude of and general characteristics of various effects.

Passive margin seismicity due to deglaciation would occur on recently deglaciated margins, and could show a variation in mechanism across the margin (Table 1). These effects are observed in Baffin Bay. The extent to which deglaciation flexure could be considered significant for passive margin seismicity depends on whether these effects are observed on other margins as, through time, the seismicity data base accumulates. Even if deglaciation is a significant effect, it is worth bearing in mind (as discussed next) that other stress sources are also operative on passive margins. Quinlan's [1984] analysis suggests that deglaciation, though adequate to trigger earthquakes, should not itself control mechanism types.

3. Spreading stresses

A second source of stress at continental margins arises from the lower density of continental crust with respect to the mantle. As a result, the continental crust tends to spread out over the oceanic lithosphere. Tensional stress in the continent, and compressional stress in the oceanic lithosphere, result [Bott, 1971; Artyushkov, 1973]. Following Turcotte and Schubert [1982] we assume for simplicity that the continental crust has density ρ_{cc}, elevation above sea level h_e, and extends to the Moho depth h_{cc}. Beneath the ocean, of depth h_w and density ρ_w, the oceanic crust has density ρ_{oc} and extends to Moho depth h_{oc}. The mantle density is ρ_m and the pressure, at depth z below sea level is

$$P_c(z) = g\,\rho_{cc}(h_e+z) \qquad (0<z) \tag{7}$$

in the continent. In the oceanic lithosphere

$$\begin{aligned} P_o(z) &= g\,\rho_w z && (z<h_w) \\ &= g\,[\rho_w h_w + \rho_{oc}(z-h_w)] && (h_w<z<h_w+h_{oc}) \\ &= g\,[\rho_w h_w + \rho_{oc} h_{oc} + \rho_m(z-h_w-h_{oc})] && (h_w+h_{oc}<z)\ . \end{aligned} \tag{8}$$

The continental Moho depth h_{cc} can be specified or, assuming isostasy, found as the depth where the pressures are equal

$$h_{cc} = \frac{(\rho_m-\rho_w)}{(\rho_m-\rho_{cc})}h_w + \frac{(\rho_m-\rho_{oc})}{(\rho_m-\rho_{cc})}h_{oc} + \frac{\rho_{cc}}{(\rho_m-\rho_{cc})}h_e\ . \tag{9}$$

The spreading stress can be estimated from the net force difference found by integrating the pressures on either side of the margin down to the depth of compensation (here h_{cc})

$$F = -h_l\Delta\bar{\sigma}_{xx} = F_c(h_{cc}) - F_o(h_{cc}) = \int_{-h_e}^{h_{cc}} P_c(z)dz - \int_{0}^{h_{cc}} P_o(z)dz \tag{10}$$

$$\begin{aligned} &= g\,[h_w h_{cc}(\rho_m-\rho_w) - h_w h_{oc}(\rho_m-\rho_{oc}) - h_w^2(\rho_m-\rho_w)/2 - h_{oc}^2(\rho_m-\rho_{oc})/2 \\ &\quad + h_{oc}h_{cc}(\rho_m-\rho_{oc}) - h_{cc}^2(\rho_m-\rho_{cc})/2 + h_e^2\rho_{cc}/2 + h_e h_{cc}\rho_{cc}]\ . \end{aligned}$$

The average stress difference $\Delta\bar{\sigma}_{xx}$ is minus the force difference, divided by the depth over

which it acts, presumably the thickness of the mechanically strong part of the lithosphere h_l. Since F is positive, the continent is in tension (negative stress) relative to the oceanic lithosphere for the pressures to be equal.

Graphically (Figure 5) the pressure at depth in the continent exceeds that in the oceanic lithosphere down to the depth of compensation, where the two are equal. The shaded area represents the integral of the difference in pressure forces, which gives rise to the stress. The stress difference is enhanced by the presence of topography, since the depth of compensation and hence the integral of the force difference increase. Sediments at the margin can be incorporated either by adjusting the crustal density, or adding more layers.

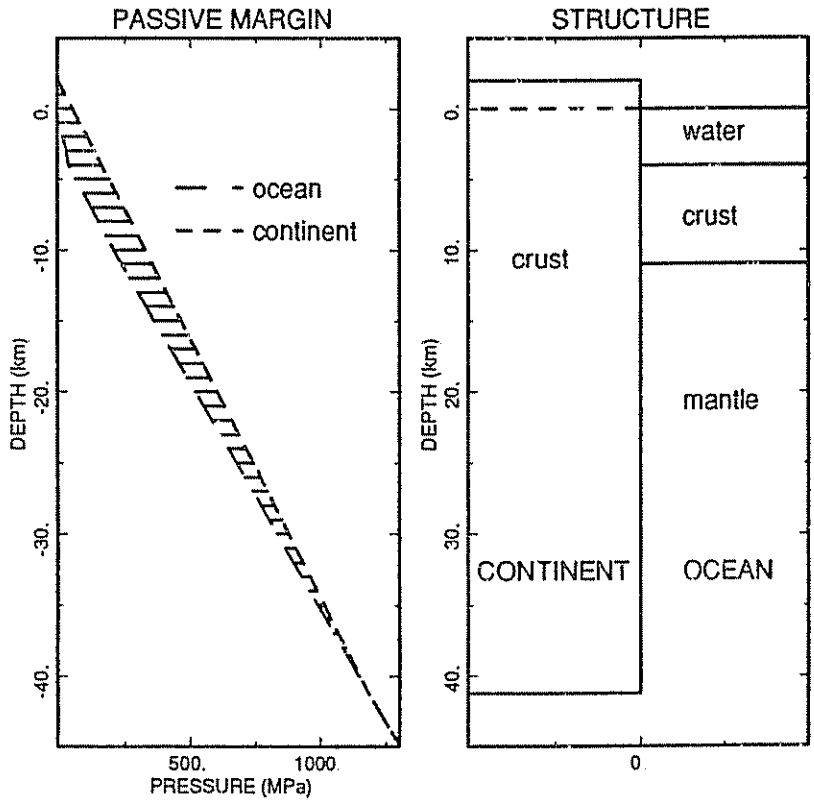

Figure 5: Schematic model for spreading stress at continental margins due to different density structures of continental crust and oceanic lithosphere. The spreading stress can be estimated from the net force difference (shaded) found by integrating the pressures on either side of the margin down to the depth of compensation, and averaging over depth.

Figure 6 shows these stresses, computed numerically for density structures approximately those observed in Baffin Bay [Reid and Falconer, 1982]. The finite difference calculation [Sleep et al., 1988] allows the stress at each depth, rather than only the vertically averaged stress, to be found. The stress is a few tens of MPa, changing from tension to compression across the margin. This calculation is a two dimensional one, but for a three dimensional calculation [Dahlen, 1982] stress should still be approximately normal to the margin. These stresses may also contribute to the Baffin Bay seismicity, but seem unlikely to provide the major effect operative, since such stresses occur on all continental margins and thus make it difficult to explain why earthquakes seem more common on recently deglaciated margins. Figures 7 and 8 illustrate the combined effect of spreading and deglaciation stresses for the Baffin Bay region.

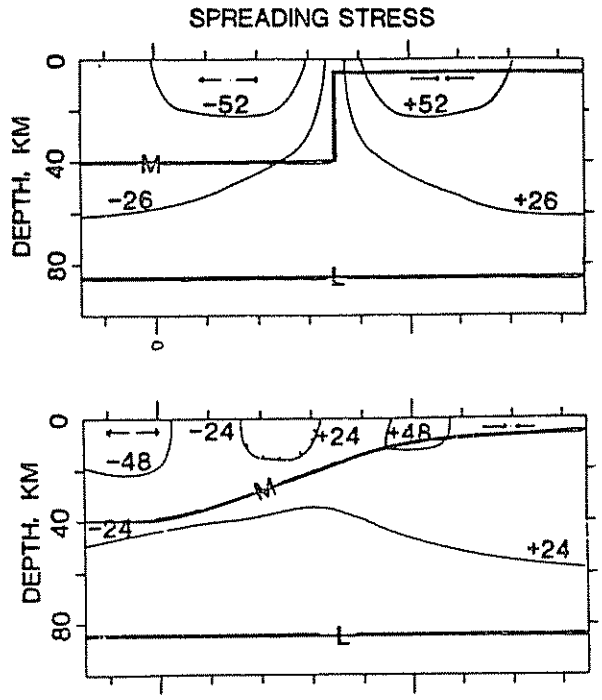

Figure 6: Deviatoric stress due to spreading at continental margin computed numerically for density structures approximately those observed in Baffin Bay. Base of lithosphere and Moho denoted by "L" and "M". Tic marks indicate 20 km distance.

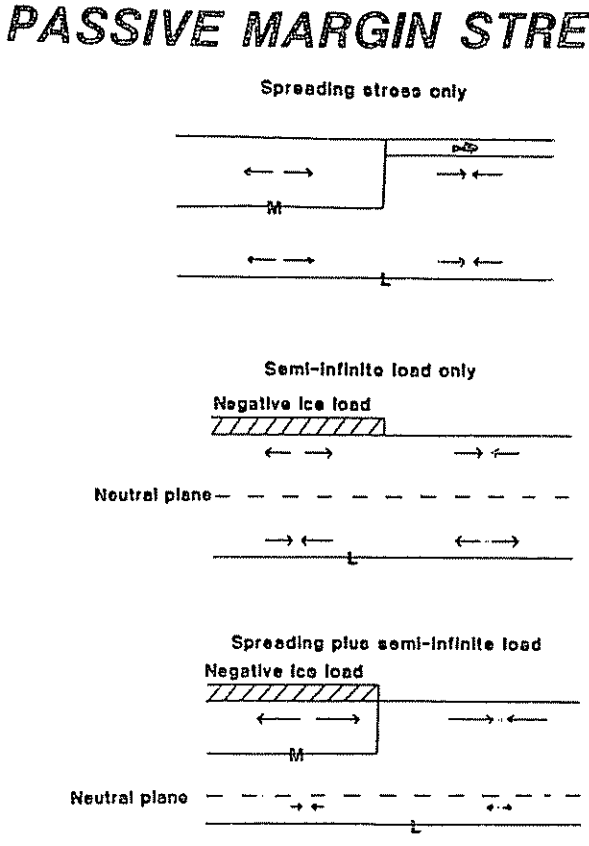

Figure 7: Schematic illustration of horizontal stress due to the effects of combining the spreading and deglaciation stresses for the Baffin Bay region [Sleep et al., 1988]. Spreading stress produces tension in the continental lithosphere and compression in the oceanic lithosphere. Removal of the ice load produces shallow tension in continental lithosphere and shallow compression in oceanic lithosphere; the stresses at depth reverse. The combination interact constructively at shallow depth and destructively at deeper depth.

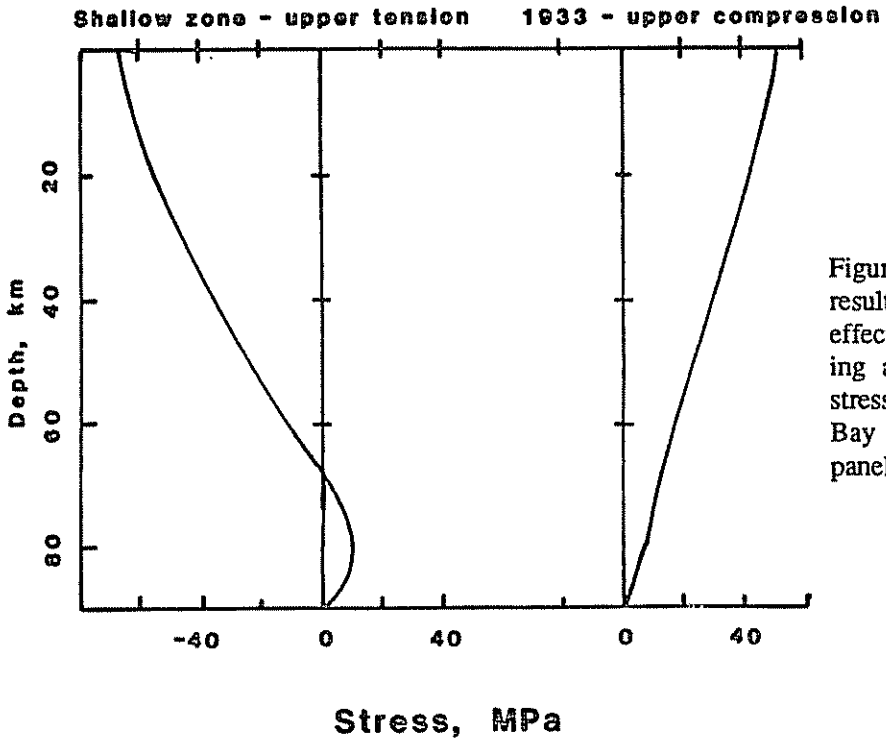

Figure 8: Numerical results for combined effects of the spreading and deglaciation stresses for the Baffin Bay region (bottom panel, Figure 7)

4. Plate driving stresses

The state of stress at a continental margin can include plate wide stresses as well as those arising at the margin itself. For the oceanic lithosphere, these stresses can be inferred from calculations of plate driving and resistive forces [Wortel and Cloetingh, 1983], including the ridge push force due to lithospheric cooling [Lister, 1975; Parsons and Richter, 1980]. The net ridge push force in the spreading direction for lithosphere of age t can be estimated as

$$F_R(t) = \alpha_v \rho_m T_m g \kappa t \qquad (11)$$

where α_v is the coefficient of thermal expansion, ρ_m and T_m are the density and temperature at the isotherm assumed to define the base of the plate, and κ is the thermal diffusivity. This force is zero at the ridge and increases linearly with age. Figure 9 illustrates the corresponding stress, averaged over the plate thickness, for various values of the basal drag coefficient. The average stress expected in oceanic lithosphere at a passive margin is thus a few tens of MPa.

Such two dimensional calculations, with force and stress varying only with distance from the ridge, have been extended to realistic plate geometries numerically by treating the ridge push as concentrated at the spreading axis [Richardson et al., 1979], and later by incorporating the ridge push as the horizontal pressure gradient integrated over the plate area [Wortel and Cloetingh, 1981; Richardson and Cox, 1984; Cloetingh and Wortel, 1985]. The results indicate that, since passive continental margins and seafloor isochrons often approximately parallel spreading axes, the predicted stresses from ridge push are often essentially normal to the margins [Richardson et al., 1979]. (This need not be the case, but is for the common Atlantic-type geometry). Within continental interiors, stress fields [Zoback et al., 1984; also several papers in this volume] often have a generally consistent orientation according with that predicted. Platewide stresses should thus contribute significantly at passive margins. As for the spreading stress, they would contribute at all passive margins, and thus do not, alone, explain the apparently higher

level of seismicity in Atlantic Canada. These stresses will also vary slowly with position and thus cannot, alone, generate closely spaced tension and compression. A final point worth noting is that the stress can include transient effects due to, for example, changes in plate geometry. Such stress variations at passive margins may be observable in subsidence records [Cloetingh et al., 1985].

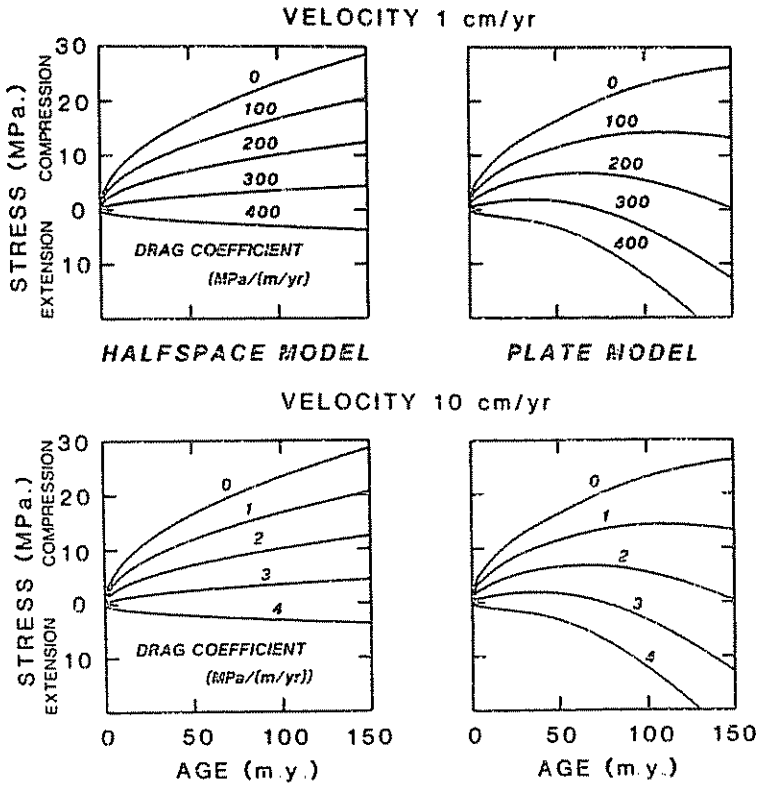

Figure 9: Numerical results for vertically averaged stress in spreading direction due to the combined effects of plate driving forces, ridge push and basal drag, as a function of plate velocity, age, and basal drag coefficient. For no drag, since plate thickness increases as the square root of age, the average stress varies as the ratio of ridge push to thickness, or also as the square root of age [Wiens and Stein, 1985].

5. Sediment load stresses

A further source of stress at passive margins is the sediment load, often in excess of 10 km (Figure 10) [Walcott, 1972, Turcotte et al., 1977; Cloetingh et al., 1983].

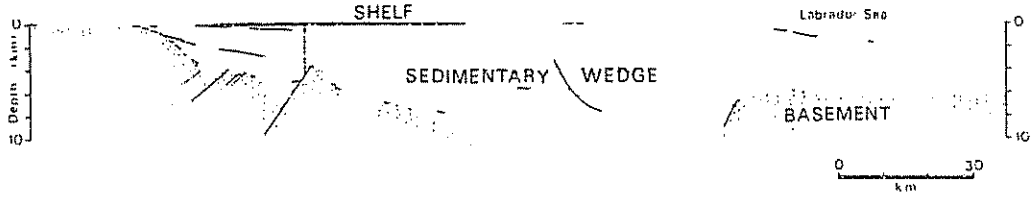

Figure 10: Cross section across the Labrador Sea margin (southern Saglek Basin) showing sedimentary prism geometry [Balkwill, 1987].

Figure 11 (top) shows the flexural stress computed for an elastic rheology, as discussed earlier, for a schematic passive margin load of 10 km of sediment deposited under water. The load half width is taken as 150 km; since the solution is formed as a Fourier cosine series, the

load and response are symmetric about the origin. For the values chosen, the deflection due to the load reaches approximately 2/3 of the isostatic, and the flexural stresses reach several hundred MPa. The sediment load accumulates during the margin's evolution: Figure 11 (bottom) shows the evolution of the deflection and stress for a simple passive margin loading history $\psi(t) = 1 - e^{-t/t_p}$, with a load rise time t_p of 50 My [Cloetingh et al., 1983]. For an elastic rheology, the deflection and stress accumulate the same way as the load, so the the final response is the same as when the load is applied instantaneously.

The stresses predicted are an order of magnitude greater than those expected from deglaciation, continent-ocean spreading, or ridge push and basal drag. Such stresses might then be expected to dominate the others, giving rise to seismicity along all passive margins, with no preference for deglaciated ones. Similarly, local variations in sediment loading, especially when coupled with the variation in the geometry of the margin, should mask the effects of the other stress sources for a considerable distance on either side of the load.

TABLE 1: POSSIBLE STRESS SOURCES AT PASSIVE MARGINS

Type	Magnitude	Direction	Spatial variation	Depth Variation	Location
Deglaciation flexure	10 MPa	essentially margin - normal	continent - extension; ocean - compression	reverses	deglaciated margins
Continental margin spreading	10 MPa	essentially margin - normal	continent - extension; ocean - compression	monotonic	all margins
Ridge push/ basal drag	10 MPa	variable, but often essentially margin - normal	compression	monotonic	all margins
Sediment flexure	100 MPa	essentially margin - normal	continent - extension; ocean - compression	reverses	all margins

The table summarizes the order of magnitude (for an elastic rheology) and characteristics of possible stress types. Different effects cause different variations in stress both spatially, presumably manifest in focal mechanism types, but also in depth, an effect in principle testable with focal depths. Although the seismicity data now available are limited, since large passive margin earthquakes are infrequent, the situation should improve as regional networks provide data on earthquakes smaller than studied with global networks. Results reported in this volume thus offer valuable prospects.

The remainder of this paper focuses on the apparent paradox that sediment loads should be the primary cause of stresses at passive margins. Discussion of two possible explanations, though far from resolving the issue, does identify useful features of the different models.

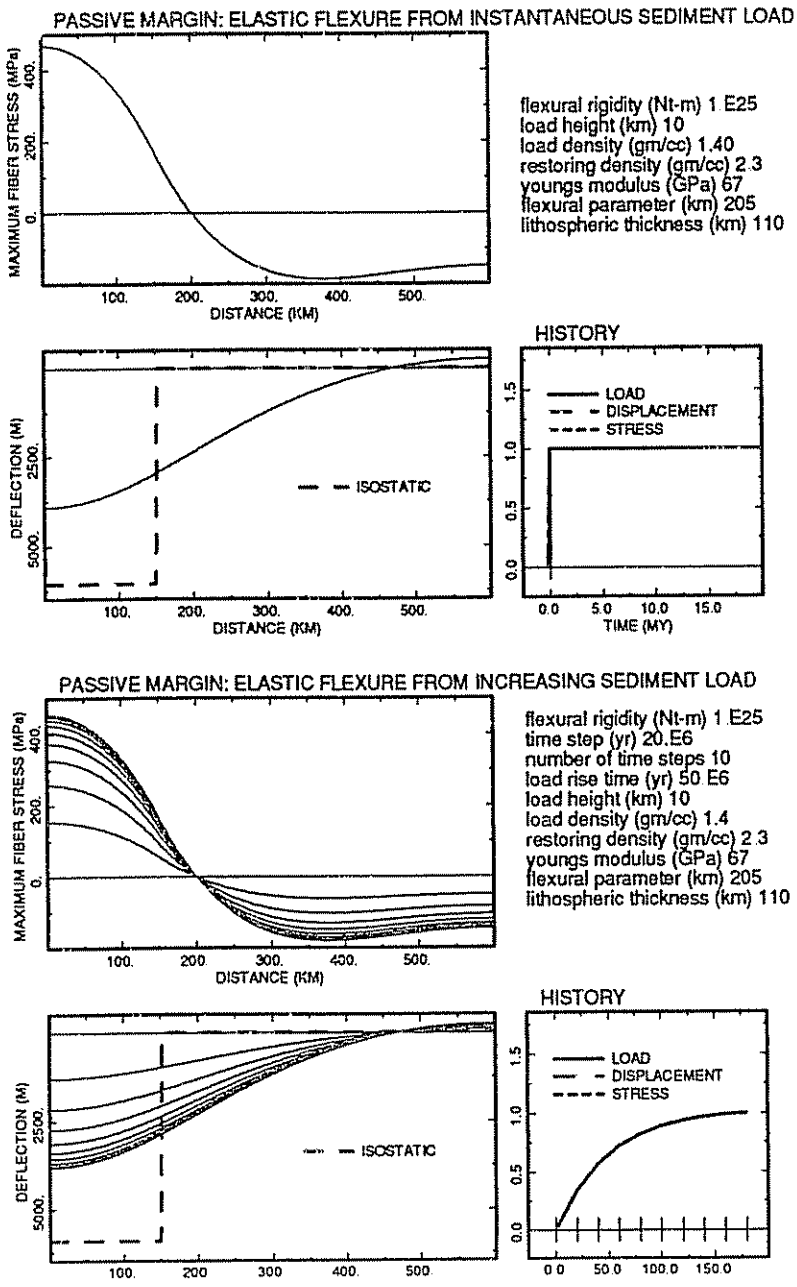

Figure 11: Flexural deflection and stress for sediment load on elastic lithosphere. Figures show the deflection at each time step and that expected for the final load from local isostasy (dashed). Flexural stress at the top of the lithosphere (compression positive) shown at each time step. History plots show the deflection, stress, and load height, normalized to their maximum values. Tic marks indicate the time samples plotted in the stress and deflection plots. *Top*: Load instantaneously applied at time zero. *Bottom*: Load applied as a function of time, corresponding to a schematic passive margin loading history.

6. Viscoelastic model

In an earlier treatment of passive margin seismicity, Stein et al. [1979] suggested that deglaciation could induce passive margin seismicity, if the large stresses from sediment loading had relaxed. Such effects are commonly modeled by assuming that the lithosphere has a viscoelastic response, in which the initial response to an applied stress is elastic, and the long term response is that of a Newtonian viscous fluid. The essential feature of such models is that the lithosphere is stronger on short time scales than on longer ones.

Walcott [1970] compared the response of the lithosphere to loads applied at various times, suggested that the apparent flexural rigidity decreased with load age, and modeled this effect for a line load on a viscoelastic lithosphere. Subsequent studies used viscoelastic models to describe the response of the lithosphere to loads including continental margins [Sleep and Snell, 1976], seamounts [Watts, 1978; Lambeck and Nakiboglu, 1981], and sedimentary basins [Beaumont, 1978; 1981; Schedl and Wiltschko, 1984]. In addition, viscoelastic models are used to describe the earth's response (primarily controlled by the lower viscosity material beneath the lithosphere) to deglaciation [Peltier, 1974; 1988; and this volume].

Here, we use a simple model in which the lithosphere is treated as a viscoelastic layer of thickness T underlain by a fluid substratum [Nadai, 1963]. The displacement $w(x,t)$ and strain $\varepsilon(x,t)$ are treated as time dependent entities having elastic and viscous parts

$$w(x,t) = w_E(x,t) + w_V(x,t) \qquad \varepsilon(x,t) = \varepsilon_E(x,t) + \varepsilon_V(x,t) \tag{12}$$

related by

$$\dot{\varepsilon}_E(x,t) + \varepsilon_E(x,t)/\tau = \dot{\varepsilon}(x,t) \tag{13}$$

where the dot indicates time differentiation. The viscoelastic behavior is characterized by τ, the Maxwell relaxation time, which Nadai defines as $3\mu/E$, three times the ratio of the viscosity to Young's modulus. (The precise form of this definition varies between authors.)

For such a material, Nadai shows that the time dependent flexural deflection $w(x,t)$ due to a line load $P(x,t)$ can be found by solving

$$D\frac{\partial^4 \dot{w}}{\partial x^4} + k(\dot{w} + \frac{w}{\tau}) = (\dot{P} + \frac{P}{\tau}), \tag{14}$$

the viscoelastic equation equivalent to (1) derived using the correspondence principle relating elastic and viscoelastic solutions. The material is assumed to be incompressible ($\nu = 1/2$), so the flexural rigidity is $D = ET^3/9$. For a load described by

$$P(x,t) = P_0 \sum_{n=0}^{\infty} \psi(t)\, C_n \cos(n\pi x/a) \tag{15}$$

with time history $\psi(t) = 1 - e^{-t/t_p}$ $(t>0)$, the displacement is

$$w(x,t) = (P_0/k) \sum_{n=0}^{\infty} \phi_n(t)\, C_n \cos(n\pi x/a) \tag{16}$$

where

$$\phi_n(t) = [(t_p - \tau)(1 - e^{-t/t_p}) - (t_n - \tau)(1 - e^{-t/t_n})] / (t_p - t_n) \tag{17}$$

and each Fourier term has characteristic time

$$t_n = [1 + (D/k)(n\pi/a)^4]\,\tau \ . \tag{18}$$

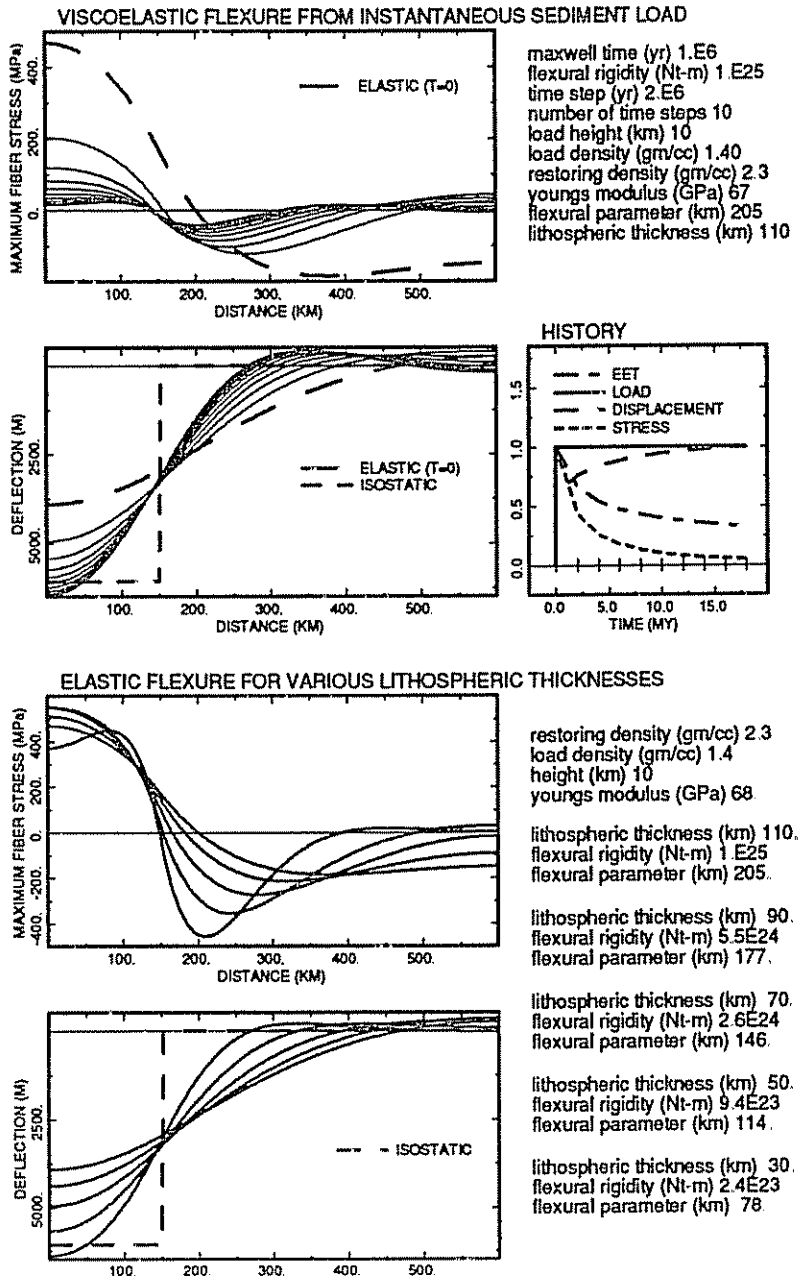

Figure 12: *Top:* Flexural deflection and stress for sediment load (same as Figure 11 (top)) on viscoelastic lithosphere. The format is the same as Figure 11, except that the history plot also shows effective elastic thickness. At time zero, the response is the same as for the elastic lithosphere. *Bottom:* Response of an elastic lithosphere of various thicknesses to the instantaneous load applied in the upper panel. For constant Young's modulus the thinner lithospheres correspond to lower rigidities and flexural parameters, and thus deeper and narrower deflections. Comparison with the deflection of the viscoelastic lithosphere with time since loading illustrates the apparent weakening of the lithosphere.

Figure 12 (top) illustrates this response, for the instantaneously applied ($t_p = 0$) sediment load in Figure 11 (top). Immediately after loading, the lithosphere responds elastically, giving the same response as in Figure 11. The load relaxes with time, eventually approaching the isostatic response. The time history panel of the figure shows the load, displacement, and stress histories; all are normalized by their maximum value.

The flexural stress, resulting from the elastic portion of the strain, also evolves with time. This is found from the elastic portion of the strain, using the integral of (9)

$$\epsilon_E(x,t) = \epsilon(x,t) - \frac{e^{-t/\tau}}{\tau} \int_0^t \epsilon(x,t') e^{t'/\tau}\, dt' \tag{19}$$

such that initially the elastic strain is the total strain. Thus the flexural stress at a vertical distance z above the neutral surface ($T/2$) is

$$\sigma_{xx}(x,z,t) = (4EzP_0 / 3k) \sum_{n=0}^{\infty} (n\pi/a)^2 f_n(t)\, C_n \cos(n\pi x/a) \tag{20}$$

where

$$f_n(t) = \tau/(t_p - t_n) \left[e^{-t/t_p} - e^{-t/t_n} \right] . \tag{21}$$

The stress (plotted at the top of the lithosphere) decays with time from the elastic value.

The deflection and stress relax on a time scale controlled by the ratio of time since loading to the Maxwell time. In our examples we generally use a Maxwell time of 1 My, or a viscosity approximately 7×10^{23} Pa-s, values comparable to those in previous studies [Sleep and Nunn, 1980]. The deflection from the instantaneous load shown in Figure 12 (top) reaches the isostatic value in approximately 10 My (ten Maxwell times).

The weakening of the lithosphere with time since loading is shown by comparison of the deflection of the viscoelastic lithosphere (Figure 12, top) with deflections computed for the same load on an elastic lithosphere of various rigidities (Figure 12, bottom). If the viscoelastic lithosphere were treated as elastic, its apparent flexural rigidity D_{app} would initially equal the true value, but is reduced as the load relaxes. The same idea can be described in terms of the effective elastic thickness of the lithosphere, which in this example is reduced by almost 75%, from 110 km to 35 km. This effect is indicated in the load history plots for the viscoelastic cases by the "EET" curves. These can be estimated either by comparing figures like the two portions of Figure 12, or by using equations (6) and (20)

$$\phi_n(t) = 1 / [\, 1 + (D_{app} / k)(n\pi/a)^4 \,] \tag{22}$$

to find D_{app} for each Fourier term, and averaging.

As noted by Beaumont [1978], the relaxation rate depends on the load size. Figure 13 illustrates this effect for a narrower load with half width 25 km: after twenty Maxwell times the deflection is 28% of the isostatic, and even after 200 Maxwell times the deflection is only 47% of the isostatic. The broad extent of the sediment load is thus significant.

For our purposes, the interesting case is the accumulation of sediment with time at a passive margin. Figure 14 (top) shows the evolution of the deflection and stress on a viscoelastic lithosphere. Since the load rise time, 50 My, is long compared to the Maxwell time (1 My), the stress can relax during the loading time. As a result, the stress never exceeds 25 MPa, and is significantly less after 100 My. Thus, for this model, the stress expected at present on a passive margin is dramatically less than for the elastic models (Figure 11). The stress reduction is still significant even for a Maxwell time of 10 My (Figure 14, bottom). In this case, stress

accumulates during the initial rapid loading, but decays during most of the loading sequence, such that at the end of the loading the stress is only a few tens of MPa.

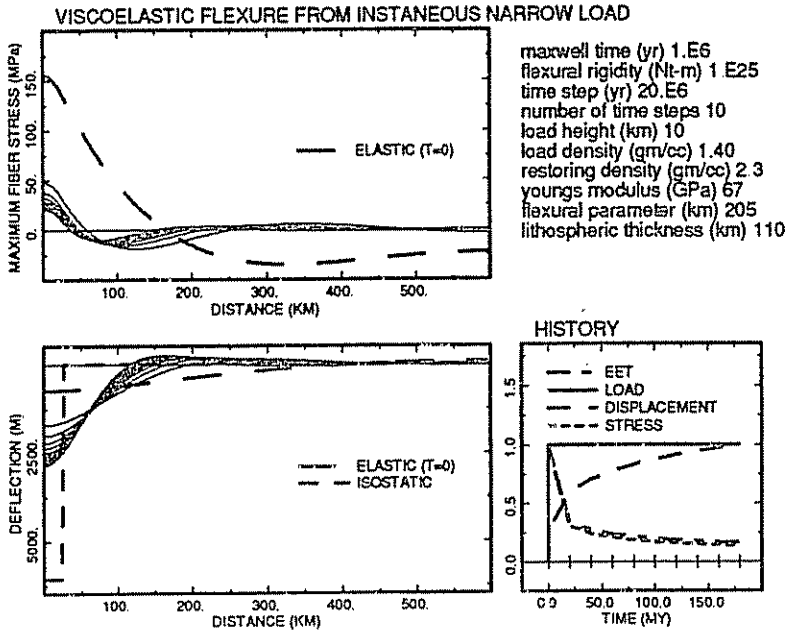

Figure 13: Flexural deflection and stress for a narrow instantaneous load, otherwise the the same as in Figure 12 *(top)*. The narrow load relaxes much more slowly.

The exponential loading solution used here is a convenience. Since the problem is linear, the solution for an instantaneous load at $t = 0$: $t_p = 0$, $\psi(t) = H(t)$

$$\phi_n(t) = 1 + (\tau/t_n - 1)\, e^{-t/t_n} \qquad f_n(t) = (\tau/t_n)\, e^{-t/t_n} \tag{23}$$

can be used to form the effects of loads at various times. Moreover, the only load solution required is that for a point load. Beaumont [1978] takes such an approach, forming a space-time convolution with the Heaviside-Green function in cylindrical coordinates.

For the passive margin loading history, the stresses that accumulate assuming a viscoelastic rheology are considerably smaller (less than 10%) than those that would develop for an elastic rheology. The situation can be quite different for more rapid loading rates. Nunn [1985] has suggested that for the northern coast of the Gulf of Mexico, where sedimentation rates are extremely high (~ 1.5 mm/yr), the loading rate is high enough to generate significant stresses and minor seismicity [Frolich, 1982]. In contrast, the loading rate in Figure 14 averaged over the load rise time is an order of magnitude slower, ~.1 mm/yr.

To examine this issue, we simulated several time histories that result in the accumulation of 1 km of sediment. Figure 15 shows the deflection and stress for an exponential time history simulating a rapid (1.5 mm/yr) sedimentation rate, for an elastic (top) and viscoelastic (bottom) lithosphere. For this rapid loading rate, stress in the viscoelastic case increases with time, as in the elastic one. The loading is rapid enough that the stress builds up, reaching 80% of the value for the elastic case. In contrast, for moderate (.5 mm/yr) and slow (.1 mm/yr) sedimentation rates (Figure 16), the loading rate is low compared to the Maxwell time. For example, in the slow case, the stress relaxes faster than it accumulates so the maximum stress reached is only about 20% of that for the elastic rheology. Moreover, the stress history shows that, rather than continuing to grow as the load does, the stress reaches steady state and eventually begins to relax even during the loading.

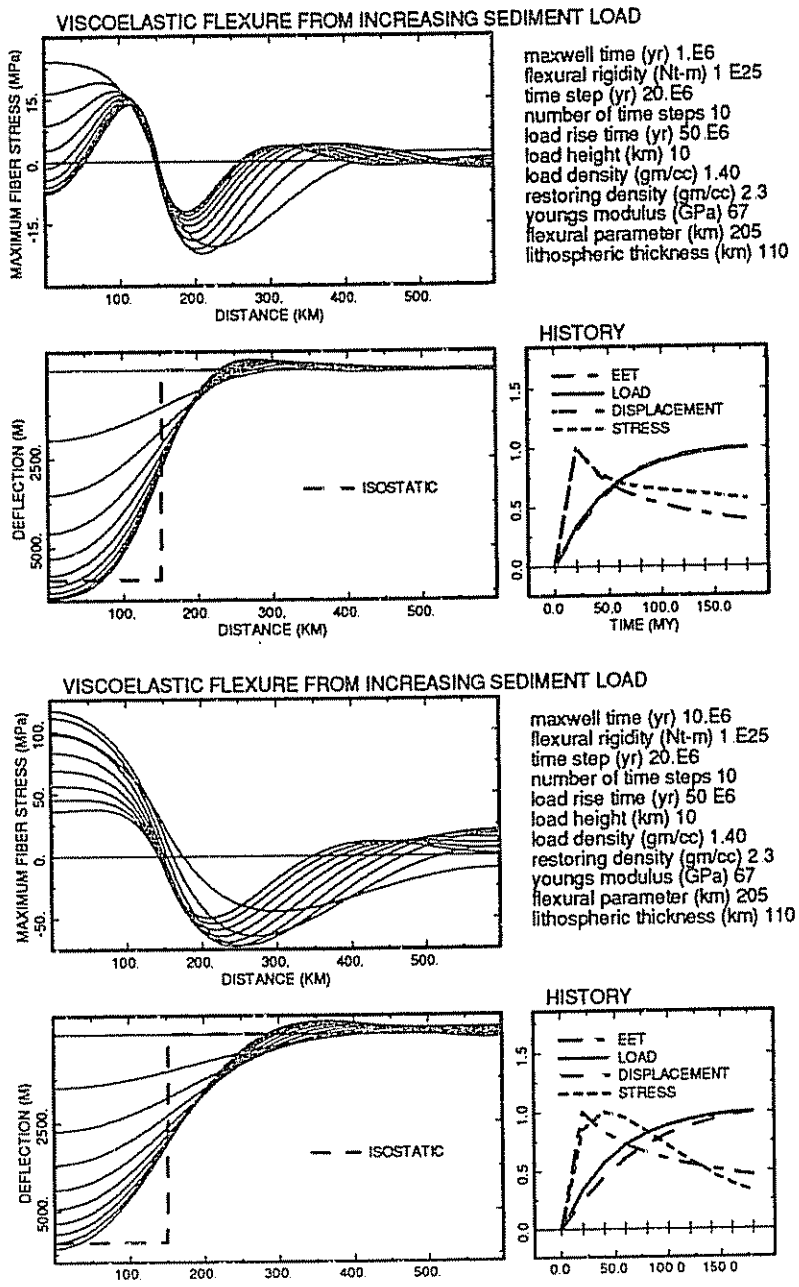

Figure 14: Flexural deflection and stress for the accumulation of sediment with time on a viscoelastic lithosphere with Maxwell times 1 My *(top)* and 10 My *(bottom)*. Since the rise time (50 My) for passive margin loading is long compared to the Maxwell times, the stress can partially relax during the loading and additional subsidence occurs. For this model, the stress is significantly less than for the same load on an elastic lithosphere (Figure 11).

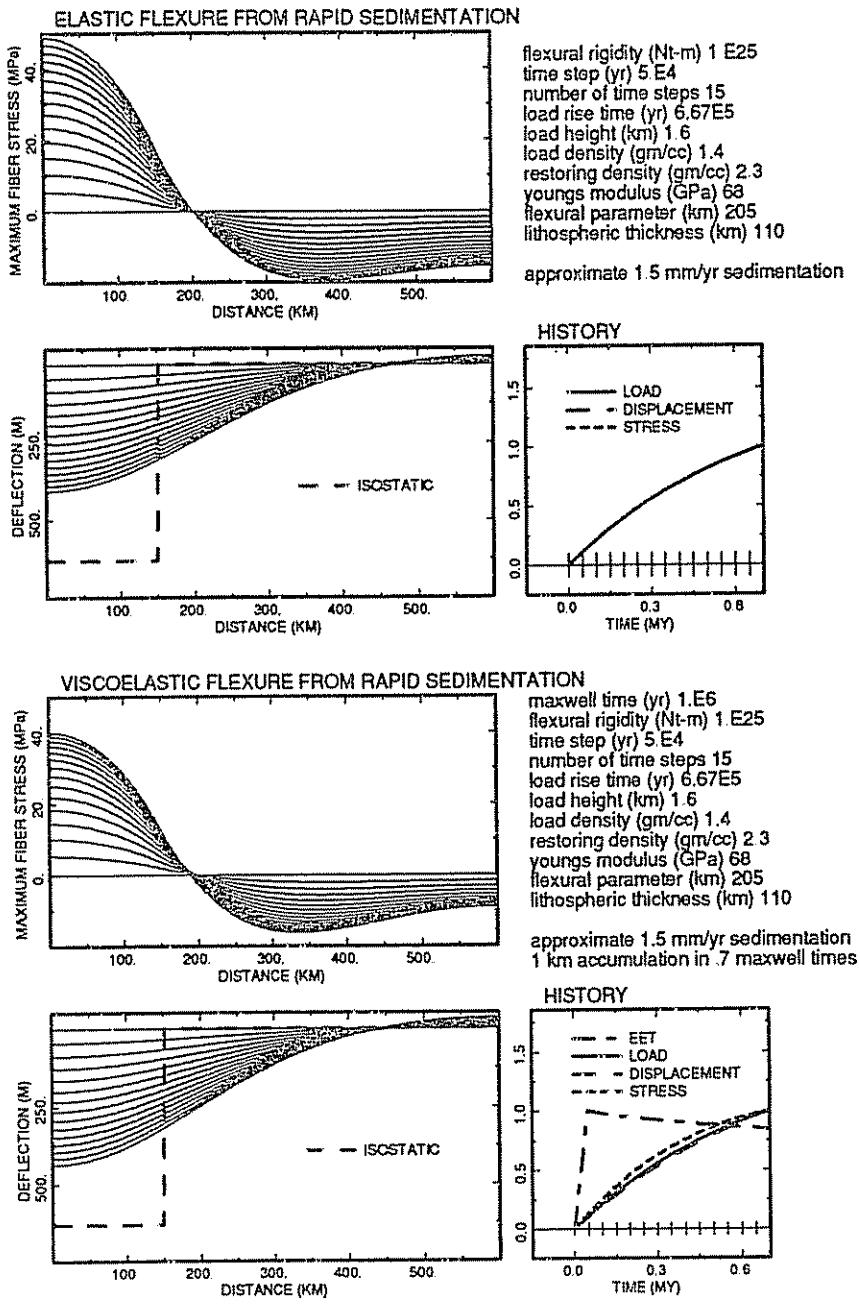

Figure 15: Flexural deflection and stress for the accumulation of sediment with time on an elastic *(top)* and viscoelastic (Maxwell time 1 My) *(bottom)* lithosphere. The load history simulates a 1.5 mm/yr sedimentation rate, rapid enough that the viscoelastic response is similar to the elastic one.

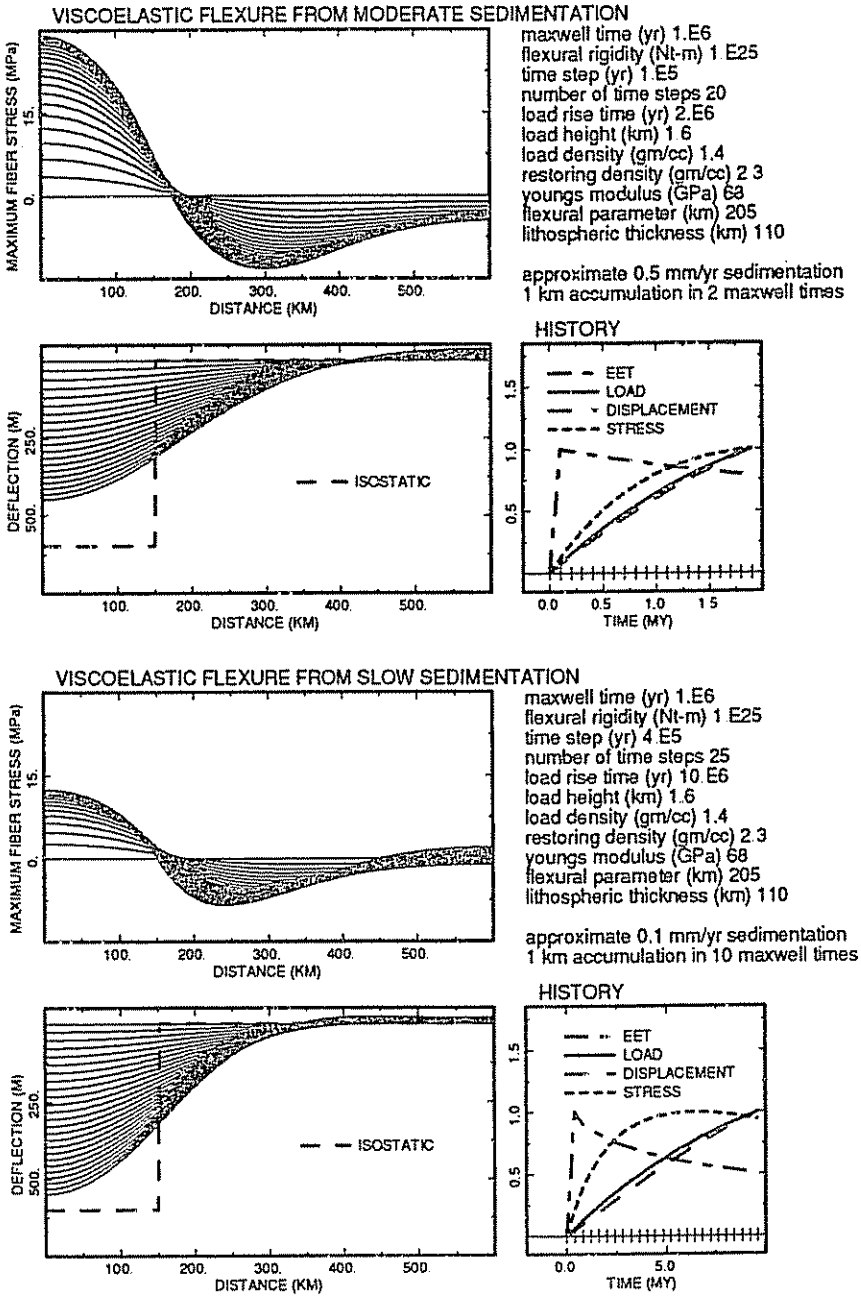

Figure 16: Flexural deflection and stress for moderate (.5 mm/yr) and slow (.1 mm/yr) sedimentation rates on a viscoelastic lithosphere. In the slow case, the stress relaxes faster than it accumulates, so the maximum stress reached is a fraction of that for the elastic rheology.

The "slow" rate used here is actually a significant one, comparable to the average rate during the first approximately 50 My of the passive margin load's accumulation. The loading rate late in the margin's evolution is much less. The effect discussed depends on the ratio of loading rate to Maxwell time; it is even more marked for shorter Maxwell times and noticeably less for much longer Maxwell times.

This simple viscoelastic model provides one mechanism by which the large sediment loads at passive margins do not generate high stresses that dominate all other stress sources. A limitation of the model is that a single viscoelastic layer, like a single elastic layer, is an oversimplification of the rheology of the lithosphere. As discussed later, the lithosphere is generally thought to be stratified into upper brittle and lower ductile regions.

Viscoelastic models, which simulate some aspects of the ductile behavior, do not replicate the brittle behavior of the upper region. In such models, the upper layer has no long term strength, a problem for large loads which relax rapidly. Composite models with upper elastic layers (or viscoelastic ones with very long Maxwell times) and lower viscoelastic layers are thus sometimes used [Peltier, 1974; Kusznir and Bott, 1977; Sleep and Nunn, 1980; Quinlan and Beaumont, 1984; Hasegawa et al., 1985]. Such models reduce the high stresses predicted for an elastic rheology [Lambeck and Nakiboglu, 1981] and simulate ductile flow in the lower lithosphere, while allowing the upper lithosphere to have finite strength over time. In such models, as stress relaxes in the lower layers, it increases in the upper ones. Viscoelastic models incorporating rheological stratification may thus be useful in analysis of passive margin loading histories. As discussed later, even further complexities result from the expected temporal variation in lithospheric rheology during the loading.

7. Brittle/ductile model

An alternative approach to the question of the sediment - induced flexural stresses is to consider models in which the lithosphere has a brittle upper region and a ductile lower one [Cloetingh et al., 1982]. Laboratory experiments on geological materials [Kirby, 1977; 1980; 1983; Goetze and Evans, 1978; Brace and Kohlstedt, 1980] suggest that these two different modes of deformation occur, at different temperature and pressure conditions. At shallow depths (low pressure and temperatures), rocks fail by brittle fracture, and strength increases with pressure and hence depth. Stresses in excess of the brittle strength are released by fracture. At greater depths (high pressures and temperatures) rocks deform by ductile flow, and strength decreases exponentially with temperature. Stresses in excess of the ductile strength are relieved by creep. This model for ductile flow describes a viscous fluid, with a temperature and strength dependent effective viscosity. Thus, as temperature increases with depth, rock strength is reduced. The combined effect of this rheology is that strength increases with depth down to the brittle - ductile transition, and decreases below it. The region with strength above a critical value (~ 25 MPa) is thus the mechanically strong part of the lithosphere (MSL).

The applicability of this model to the earth is suggested by the observations that, as the oceanic lithosphere ages and cools, the depth to the low velocity zone [Leeds et al., 1974; Forsyth, 1975], the effective elastic thickness inferred from seamount loads [Bodine et al., 1981], and the maximum depth of oceanic intraplate seismicity [Wiens and Stein, 1983; Chen and Molnar, 1983], all increase with age. Since the lithosphere cools with age, the depth variations are interpreted as reflecting the deepening of isotherms and hence of the portion of the lithosphere with strength above critical values. Thus the brittle/ductile model, though presumably an approximation to a complex reality, accounts for a wide range of observations.

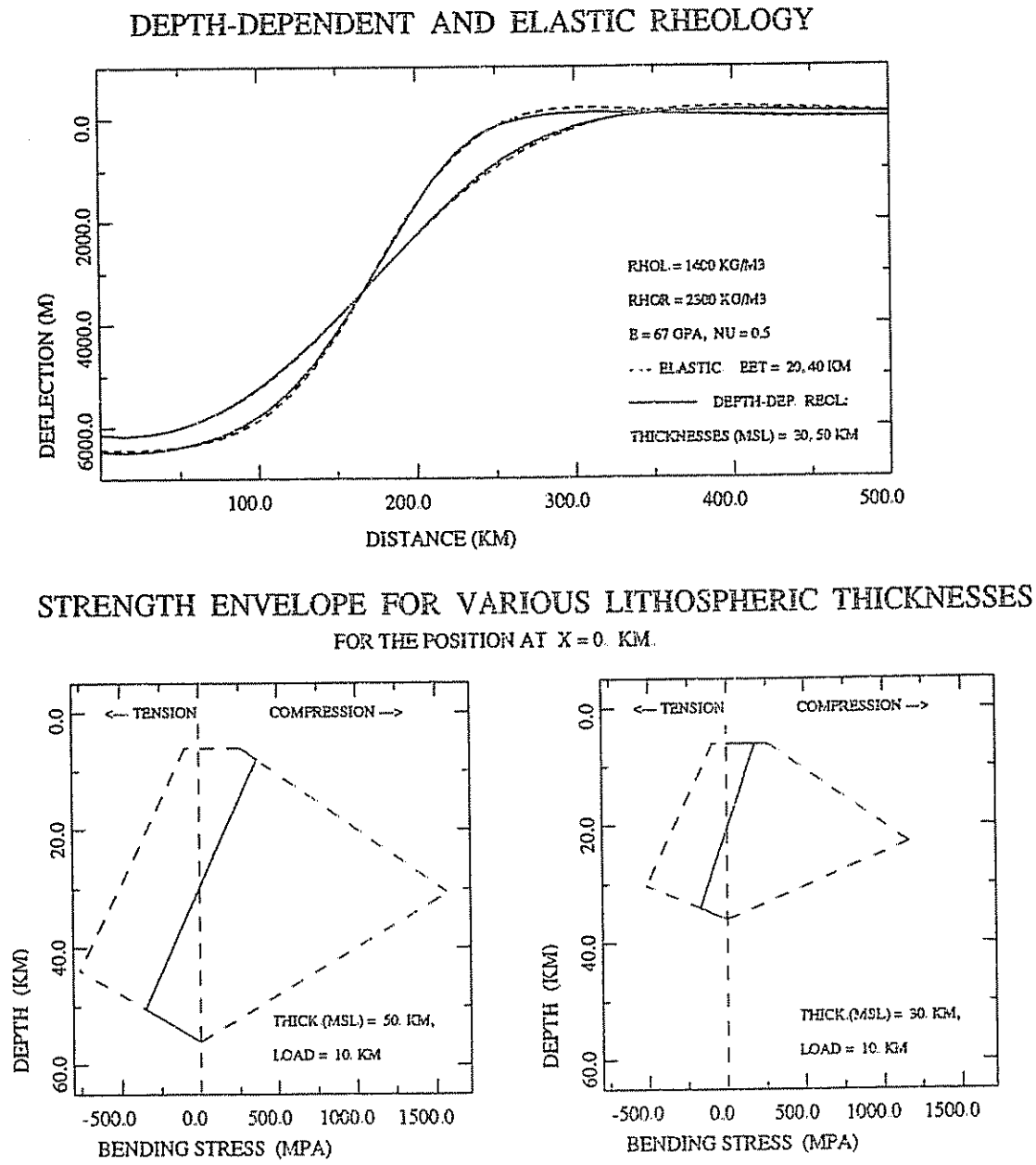

Figure 17: *Top*: Flexural deflection for 10 km thick, 150 km wide, sediment load applied on lithospheres with various rheologies. Solid lines show deflection of brittle/ductile lithospheres with 30 and 50 km thick mechanically strong parts, corresponding to 30 and 100 My old lithosphere. Dashed lines show deflection of elastic lithospheres with thicknesses of 20 and 40 km. For each rheology the weaker lithospheres give deeper and narrower deflections. Comparison of the solid and dashed curves illustrates the weakening effect of depth-dependent rheology. *Bottom*: Strength envelopes (dashed lines) for various lithospheric thicknesses, and stress distributions (solid lines) induced by flexure due to sediment loading.

For our purposes, an important feature of this model is that its strength is intermediate between elastic and viscoelastic models. In an elastic model, the lithosphere can support arbitrarily high stresses indefinitely, and so has infinite strength on all time scales. Loading a viscoelastic model gives infinite strength on a short time scale, and zero strength on a long time scale. The latter effect poses difficulties primarily for long wavelength loads, since the time required for short wavelength loads to relax can be extremely long. The brittle/ductile rheology gives at any depth, in both the brittle and ductile regions, maximum stresses that can be supported. Thus, in this model, the lithosphere has finite strength on all time scales.

The flexure produced by loading a lithosphere with a brittle/ductile rheology thus differs from those for either an elastic or viscoelastic rheology. Figure 17 (top) contrasts the deflections for lithospheres with a brittle/ductile rheology to those for elastic lithospheres. Since the finite strength results in stresses that are less than for an elastic model (Figure 17, bottom), the effective elastic thickness is less than the thickness of the mechanically strong lithosphere. For example, a 50 km thick brittle/ductile lithosphere has an effective elastic thickness of about 40 km. The calculations were done using a finite difference version of the flexural equation, allowing depth-variable strength [Bodine, 1981]. Such calculations can also be done using finite elements, which allow the rheology to vary both in depth and laterally [Cloetingh et al., 1982].

This reduction in stress does not in itself resolve the difficulty that the stresses from sediment loading would be expected to be the largest stresses at passive margins. A further assumption, however, may overcome this. To this point, we have implicitly assumed that the stress level at margins should be directly reflected in their seismicity. An alternative approach is to consider the state of stress in a lithosphere with a brittle/ductile rheology, and assume that seismicity occurs only when the stress reaches the strength for the first time. This hypothesis has been used to describe the depth variation of earthquakes in subducting slabs [Wortel, 1986; Wortel and Vlaar, 1988] and of intraplate oceanic earthquakes [Wortel and Cloetingh, 1985]. Seismicity is assumed to occur only in depth ranges where the anelastically deforming region increases at the expense of the strong elastic "core" of the mechanically strong part of the lithosphere. Thus at certain depths the stress, previously less than the strength, now reaches or exceeds it and causes earthquakes.

This concept is schematically illustrated in Figure 18. Consider oceanic lithosphere of ages 50 and 60 My subjected to a compression resulting in the stress distribution indicated by the shading. At 50 My (Figure 18a) the upper and lower parts (darker shading) fail in the brittle and the ductile mode, respectively. In the middle part stresses are supported elastically. Now consider the same lithosphere 10 My later (Figure 18b) subject to higher stresses. The strength envelope has changed, since the lithosphere strengthens as it cools. Thus, in response to the assumed higher stress, several changes in the stress distribution with depth occur:

- The stress in the elastic part of the lithosphere increases.
- The shallow depth range in which the applied stress reaches the brittle strength has increased by about 2 km. According to Wortel's [1986] hypothesis, seismicity during this 10 My interval occurs in this *incremental depth range* (dark shading).
- A very small depth range near 35 km, formerly in the ductile field at 50 My, is now in the elastic range owing to the strengthening of the lithosphere.

The interaction between the strengthening (cooling) and loading (increasing stress) rates controls whether the transition from elastic to anelastic behavior occurs. Depending on these rates, such a transition can also occur at the lower end of the strength envelope (around 35 km depth), in contrast with the situation shown in Figure 18b.

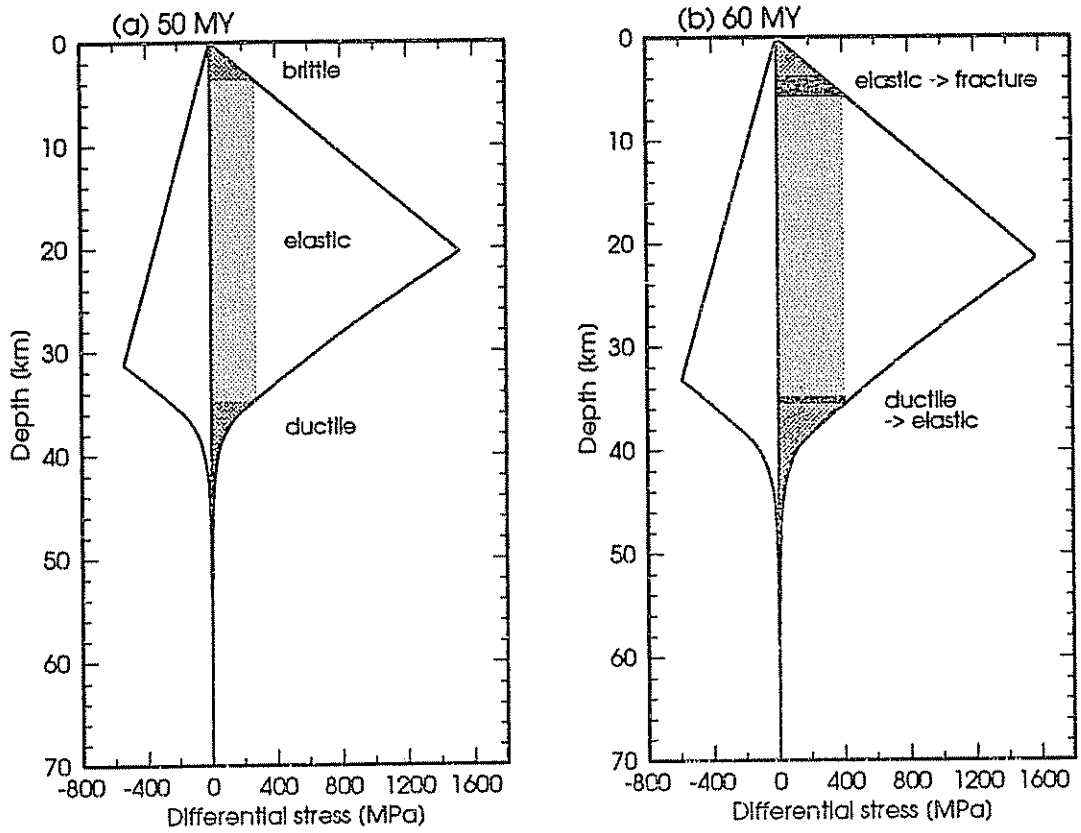

Figure 18: Schematic illustration of the relation between depth-dependent rheology, stress distribution, and seismicity [Wortel, 1986; Wortel and Cloetingh, 1986]. Compression is positive. *(a)* Strength envelope for 50 My old oceanic lithosphere. The shading gives the stress distribution, corresponding to an assumed compressive intraplate stress. The brittle, elastic, and ductile depth ranges are indicated by the different shadings.
(b) Strength envelope for the lithosphere, 10 My later. The lithosphere has strengthened, and the compressive intraplate stress is assumed to have increased. As a result, the relative values of strength and applied stress have changed in the depth ranges indicated by dark shadings (near 5 km and 35 km). Seismicity is assumed to result in the depth range in which the transition from elastic to anelastic behavior occurs.

Figure 18 illustrated the application of this model to a situation of high compressive intraplate stresses, as proposed for the Central Indian Basin [Cloetingh and Wortel, 1986]. The same approach can be applied to the response of passive margins to flexural stresses due to sediment loading. The large stresses associated with the sediment loads may have generated past seismicity, but now no longer do so. Subsequent smaller stresses derived from sources like ridge push, spreading, or deglaciation can perturb the stress field.

This discussion bears out the point that, in both this model and the viscoelastic ones, the time-dependent response of the lithosphere to loads is important for considering passive margin seismicity. Both models assume that the large stresses due to the sediment load no longer give rise to earthquakes. The situation is further complicated by the fact the rheology of the lithosphere, as well as the load applied to it, change during the evolution of the margin. Ideally, any model for this process would incorporate a model of how a time-variable load affects a time-variable lithosphere.

8. Discussion

A number of distinct mechanisms may contribute to the stress at passive margins, and thus be partially responsible for the seismicity there. If the simple models reviewed here offer a realistic general description of these mechanisms, the flexural effect of large sediment loads (assuming an elastic lithosphere) should be the dominant effect. Other stress sources should thus have smaller, perturbing, effects.

As discussed, we find this an unlikely situation for two reasons. First, there is no clear case that passive margin earthquakes are associated with the most heavily sedimented margins. There is, however, a suggestion that the larger earthquakes are most frequently associated with the deglaciated regions. Admittedly, the dataset of passive margin earthquakes is small, and may be unrepresentative due to the short length of the instrumental record and the large recurrence times of these earthquakes. Nonetheless, if either observation proves valid, it is hard to see how the sediment loading stresses can be the primary determinant of passive margin seismicity.

Second, as reported in this volume by Adams, there appears to be a consistent stress field in northeastern North America which generally agrees with the the predictions of models for stresses due to plate driving forces. These stresses should be significantly less than those due to the sediment loads. If so, it is surprising that they are not masked by the variation in sediment derived stress along the margin, at least for several hundred km inland.

We thus suggest two models that would reduce the predicted effect of the sediment load stress on passive margin seismicity. Both are based on lithospheric rheology at passive margins, and assume that an elastic model is not appropriate. This statement at first seems hardly worthy of note, given that elastic models fail to describe many aspects of lithospheric rheology. Here, however, it appears that we may have to go further. The reduction in stress implied by either of the nonelastic rheologies we consider does not alone resolve the difficulty of the sediment stress. Some mechanism depending on the load history seems necessary, such that the sediment loads do not, in general, induce most passive margin earthquakes. Both of our models thus have this feature. In the viscoelastic model, the relaxation by creep of the stress due to the sediment load qualitatively accounts for the low seismicity. It is worth noting that no explicit relation between the seismicity and stress has been formulated for a viscoelastic medium. For the brittle/ductile model, we assume that the stresses are high, but that seismicity results only when the stress in portions of the lithosphere *reaches* the strength. Seismicity is thus induced only by recent perturbations to the stress field rather than the long term sediment load. Further work along these lines

requires modelling of the evolution of the state of stress along passive margins. As a result, subsidence records and other data bearing on the history of the margins are relevant for consideration of the seismicity.

It is worth noting that both the viscoelastic and brittle/ductile models for the rheology of the lithosphere at passive margins result in a reduction of the effective elastic thicknesses of the lithosphere. Gravity data [Karner and Watts, 1982] have been interpreted as showing small effective elastic thicknesses of the lithosphere at such margins, since the initial sediment loads were applied to young, weak, lithosphere. Consideration of these data thus bears out the need to understand the response of a lithosphere whose rheology varies with time to a time varying load.

Our suggestions on the causes of passive margin seismicity are thus rather preliminary. One might argue that until the earthquake dataset for passive margin seismicity is significantly larger, few definite conclusions can be reached. Our view is that the limited dataset is adequate to suggest a variety of intriguing possibilities which a better mechanism and depth dataset could address. Moreover, consideration of possible mechanisms for passive margin seismicity leads to longstanding questions about the rheology and stress state of the lithosphere from a different perspective. An understanding of the causes of passive margin earthquakes thus may have broad implications for a variety of seemingly unrelated issues.

Finally, as discussed elsewhere in this volume, passive margin seismicity has intriguing implications for seismic hazard analysis. As noted earlier [Stein et al., 1979], if such seismicity results from reactivation of continental margin rifting faults, large earthquakes can occur anywhere along rifted margins where deglaciation, rapid sedimentation, or other effects provide the necessary stress. Given the apparent association between deglaciation and some passive margin seismicity, it would not be surprising if future large earthquakes occur along margins such as eastern Canada, the northeastern U.S., and Fennoscandia. Basham's [this volume] suggestion that the entire eastern Canadian margin be considered capable of infrequent M_s 7 earthquakes thus seems prudent. The same presumably applies to the U.S. Atlantic margin, especially the previously glaciated portions. The 1755 Cape Ann earthquake, and some of the other large preinstrumental earthquakes off the Massachusetts coast [Von Hake, 1973], may have been such events.

Acknowledgements

This research was supported by NSF grants EAR 8618038 and INT 8610654, NASA grant NAG5-885, and NATO grant 0148/87. We thank Wim Spakman for the use of his plotting program and Reinie Zoetemeijer for assistance.

REFERENCES

Artyushkov, E.V., Stresses in the lithosphere caused by crustal thickness inhomogeneities, *J. Geophys. Res., 78*, 7675-7708, 1973.

Balkwill, H. R., Labrador Basin: Structure and Stratigraphic style, in *Sedimentary Basins and Basin-Forming Mechanisms*, edited by C. Beaumont and A.J. Tankard, Can. Soc. Petrol. Geol. Memoir, 12, 17-43, 1987.

Basham, P. W., D. A. Forsyth, and R. J. Wetmiller, The seismicity of northern Canada, *Can. J. Earth Sci., 14*, 1646-1667, 1977.

Beaumont, C., The evolution of sedimentary basins on viscoelastic lithosphere: Theory and examples, *Geophys. J. R. Astron. Soc., 55*, 471-498, 1978.

Beaumont, C., Foreland basins, *Geophys. J. R. Astron. Soc., 65* 291-329, 1981.

Bodine, J. H., The thermo-mechanical properties of the oceanic lithosphere, *Ph. D. Thesis, Columbia University, New York*, 332 pp., 1981.

Bodine, J. H., M. S. Steckler, and A. B. Watts, Observations of flexure and the rheology of the oceanic lithosphere, *J. Geophys. Res., 86*, 3695-3707, 1981.

Bott, M.H.P., Evolution of young continental margins and the origin of shelf basins, *Tectonophysics, 11*, 319-327, 1971.

Brace, W. F., and D. L. Kohlstedt, Limits on lithospheric stress imposed by laboratory experiments, *J. Geophys. Res., 85*, 6248-6252, 1980.

Bungum, H., B. K. Hokland, E. S. Husebye, and F. Ringdahl, An exceptional intraplate earthquake sequence in Meloy, northern Norway, *Nature, 280*, 32-35, 1979.

Chen, W. -P., and P. Molnar, Focal depths of intracontinental and intraplate earthquakes and their implications for the thermal and mechanical properties of the lithosphere, *J. Geophys. Res., 88*, 4183-4214, 1983.

Cloetingh, S., H. McQueen, and K. Lambeck, On a tectonic mechanism for regional sealevel variations, *Earth Planet. Sci. Lett., 75*, 157-166, 1985.

Cloetingh, S., and R. Wortel, Regional stress field of the Indian Plate, *Geophys. Res. Lett., 12*, 77-80, 1985.

Cloetingh, S.A.P.L., M.J.R. Wortel, and N.J. Vlaar, Evolution of passive continental margins and initiation of subduction zones, *Nature, 297*, 139-142, 1982.

Cloetingh, S.A.P.L., M.J.R. Wortel, and N.J. Vlaar, State of stress at passive margins and initiation of subduction zones, *Am. Assoc. Petrol. Geol. Memoir, 34*, 717-734, 1983.

Dahlen, F. A., Isostatic geoid anomalies on a sphere, *J. Geophys. Res., 87*, 3943-3948, 1982.

Forsyth, D. W., The early structural evolution and anisotropy of the oceanic upper mantle, *Geophys. J. R. Astron. Soc., 43*, 103-162, 1975.

Frohlich, C., Seismicity of the central Gulf of Mexico, *Geology, 10*, 103-106, 1982.

Goetze, C., and B. Evans, Stress and temperature in the bending lithosphere as constrained by experimental rock mechanics, *Geophys. J. R. Astron. Soc., 59*, 463-478, 1979.

Gutenberg, B., and C. F. Richter, *Seismicity of the Earth and Associated Phenomena*, Princeton University Press, Princeton, N.J., 1954.

Hasegawa, H. S., J. Adams, and K. Yamazaki, Upper crustal stresses and vertical stress migration in Eastern Canada, *J. Geophys. Res., 90*, 3637-3648, 1985.

Hasegawa, H. S., C. W. Chou, and P. W. Basham, Seismotectonics of the Beaufort Sea, *Can. J. Earth Sci., 16*, 816-830, 1979.

Hashizume, M., Two earthquakes on Baffin Island and their tectonic implications, *J. Geophys. Res., 78*, 6069-6081, 1973.

Husebye, E. S., H. Bungum, J. Fyen, and H. Gjoystdal, Earthquake activity in Fennoscandia,

Norsk Geol. Tiddsk., 58, 51-68, 1978.

Kamer, G. D., and A.B. Watts, On isostasy at Atlantic-type continental margins, *J. Geophys. Res., 87*, 2923-2948, 1982.

Kirby, S. H., State of stress in the lithosphere: Inferences from the flow laws of olivine, *Pageoph., 115*, 245-258, 1977.

Kirby, S. H., Tectonic stresses in the lithosphere: Constraints provided by the experimental deformation of rocks, *J. Geophys Res., 85*, 6353-6363, 1980.

Kirby, S. H., Rheology of the lithosphere, *Rev. Geophys. Space Phys., 21*, 1458-1487, 1983.

Kuznir, N. J., and M.H.P. Bott, Stress concentration in the upper lithosphere caused by underlying visco-elastic creep, *Tectonophysics, 43*, 247-256, 1977.

Lambeck, K., and S. M. Nakiboglu, Seamount loading and stress in the ocean lithosphere 2: viscoelastic and elastic-viscoelastic models, *J. Geophys. Res., 86*, 6961-6984, 1981.

Leeds, A. R., L. Knopoff, and E. G. Kausel, Variations of upper mantle structure under the Pacific Ocean, *Science, 186*, 141-143, 1974.

Lister, C. R. B., Gravitational drive on oceanic plates caused by thermal contraction, *Nature, 257*, 663-665, 1975.

Nadai, A., *Theory of Flow and Fracture of Solids, part two*, McGraw-Hill, New York, 705 pp., 1963.

Nunn, J.A., State of stress in the northern Gulf Coast, *Geology, 13*, 429-432, 1985.

Parsons, B., and F.M. Richter, A relation between the driving force and the geoid anomaly associated with mid-oceanic ridges, *Earth Planet. Sci. Lett., 51*, 445-450, 1980.

Peltier, W. R., The impulse response of a Maxwell earth, *Rev. Geophys. Space Phys., 12*, 649-669, 1974.

Peltier, W. R., Lithospheric thickness, Antarctic deglaciation history, and ocean basin discretization effects in a global model of postglacial sea level change, in *Mathematical Geophysics*, edited by N. J. Vlaar, G. Nolet, M. J. R. Wortel, and S. A. P. L. Cloetingh, pp. 325-346, D. Reidel, Dordrecht, 1988.

Qamar, A., Seismicity of the Baffin Bay region, *Bull. Seism. Soc. Am., 64*, 87-98, 1974.

Quinlan, G., Postglacial rebound and focal mechanisms of eastern Canadian earthquakes, *Can. J. Earth Sci., 21*, 1018-1023, 1984.

Quinlan, G., and C. Beaumont, Appalachian thrusting, lithospheric flexure and the Paleozoic stratigraphy of the eastern interior of North America, *Can. J. Earth Sci., 21*, 973-996, 1984.

Reid, I., and R. K. H. Falconer, A seismicity study in northern Baffin Bay, *Can. J. Earth Sci., 19*, 1518-1531, 1982.

Richardson, R. M., and B. L. Cox, Evolution of oceanic lithosphere: a driving force study of the Nazca plate, *J. Geophys. Res., 89*, 10043-10052, 1984.

Richardson, R. M., S. C. Solomon, and N. H. Sleep, Tectonic stress in the plates, *Rev. Geophys. Space Phys., 17*, 981-1020, 1979.

Schedl, A., and D. W. Wiltschko, Sedimentological effects of a moving terrain, *J. of Geol., 92*, 273-287, 1984.

Sleep, N., G. Kroeger and S. Stein, Canadian passive margin stress field inferred from seismicity, *J. Geophys. Res.*, submitted, 1988.

Sleep, N. and J. Nunn, Flexure of a rheologically stratified lithosphere, *in* Nemat-Nassar (ed), *Solid Earth Geophysics and Geotechnology*, AMD *42*, 61-71, Am. Soc. Mech. Eng., New York, NY, 1980.

Sleep, N. H., and N. S. Snell, Thermal contraction and flexure of mid-continent and Atlantic marginal basins, *Geophys. J. R. Astron. Soc., 45*, 125-154, 1976.

Stein, S., N. Sleep, R. Geller, S. Wang and G. Kroeger, Earthquakes along the passive margin of

eastern Canada, *Geophys. Res. Lett*, *5*, 537-540, 1979.

Sykes, L. R., Intraplate seismicity, reactivation of preexisting zones of weakness, alkaline magmatism and other tectonism postdating continental fragmentation, *Rev. Geophys. Space Phys.*, *16*, 621-668, 1979.

Sykes, L. R., and M. L. Sbar, Focal mechanism solutions of intraplate earthquakes and stresses in the lithosphere, in *Geodynamics of Iceland and the North Atlantic Area*, edited by L. Kristjansson, pp. 207-224, D. Reidel, Dordrecht, 1974.

Turcotte, D.L., J.L. Ahern, and J.M. Bird, The state of stress at continental margins, *Tectonophysics*, *42*, 1-28, 1977.

Turcotte, D. L., and G. Schubert, *Geodynamics*, 450 pp., Wiley, New York, 1982.

Van Hake, C., Earthquake history of Massachusetts, *Earthq. Inf. Bull. U.S. Dept. Int*, *Geol. Surv*, *5 (5)*, 22-24, 1973.

Walcott, R. I., Isostatic response to loading of the crust in Canada, *Can. J. Earth Sci.*, *7*, 716-727, 1970.

Walcott, R. I., Gravity, flexure and the growth of sedimentary basins at a continental edge, *Geol. Soc. Am. Bull.*, *83*, 1845-1848, 1972.

Watts, A. B., An analysis of isostasy in the world's oceans, 1 Hawaiian Emperor seamount chain, *J. Geophys. Res.*, *83*, 5989-6004, 1978.

Wiens, D. A., and S. Stein, Age dependence of oceanic intraplate seismicity and implications for lithospheric evolution, *J. Geophys. Res.*, *88*, 6455-6468, 1983.

Wiens, D. A., and S. Stein, Implications of oceanic intraplate seismicity for plate stresses, driving forces and rheology, *Tectonophysics*, *116*, 143-162, 1985.

Wortel, R., Deep earthquakes and the thermal assimilation of subducting lithosphere, *Geophys. Res. Lett.*, *13*, 34-37, 1986.

Wortel, R., and S. Cloetingh, On the origin of the Cocos-Nazca spreading center, *Geology*, *9*, 425-430, 1981.

Wortel, R., and S. Cloetingh, A mechanism for the fragmentation of oceanic plates, *Am. Assoc. Petrol. Geol. Memoir*, *34*, 793-801, 1983.

Wortel, R., and S. Cloetingh, Seismic energy release and stress in the lithosphere, *Terra Cognita*, *6*, 323, 1986.

Wortel, M. J. R., and N. J. Vlaar, Subduction zone seismicity and the thermo-mechanical evolution of downgoing lithosphere, *Pageoph.*, in press.

Zoback, M. L., M. D. Zoback, and M. E. Schiltz, Index of stress data for the North American and parts of the Pacific Plate, *U. S. Geol. Surv. Open-File Report*, *84-157*, 1984.